IEEE Photonics Journal
An IEEE Photonics Society Publication

Open Access

Spectral Characteristics of Plasmonic Metal–Insulator–Metal Waveguides With a Tilted Groove

Volume 4, Number 5, October 2012

Kun-Hua Wen
Lian-Shan Yan, Senior Member, IEEE
Wei Pan, Member, IEEE
Bin Luo, Member, IEEE
Zhen Guo
Ying-Hui Guo
Xian-Gang Luo, Senior Member, IEEE

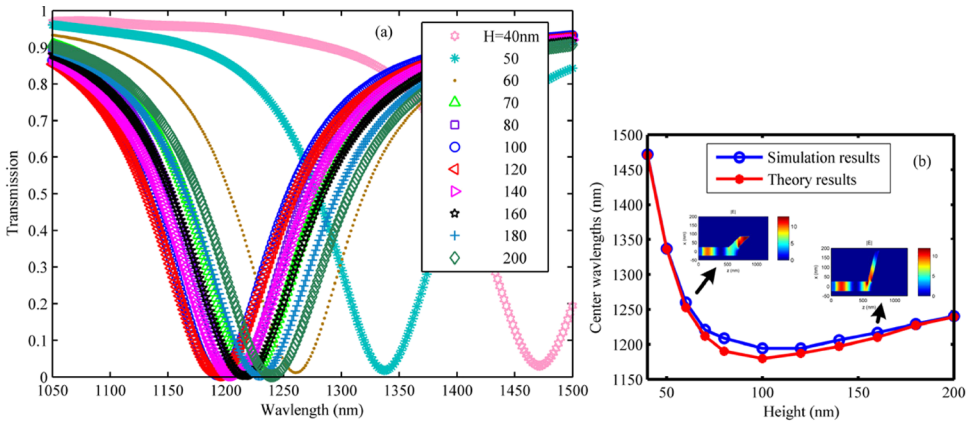

DOI: 10.1109/JPHOT.2012.2216863
1943-0655/$31.00 ©2012 IEEE

Spectral Characteristics of Plasmonic Metal–Insulator–Metal Waveguides With a Tilted Groove

Kun-Hua Wen,[1] Lian-Shan Yan,[1] *Senior Member, IEEE*, Wei Pan,[1] *Member, IEEE*, Bin Luo,[1] *Member, IEEE*, Zhen Guo,[1] Ying-Hui Guo,[1] and Xian-Gang Luo,[2] *Senior Member, IEEE*

[1]Center for Information Photonics & Communications, School of Information Science and Technology, Southwest Jiaotong University, Chengdu 610031, China
[2]State Key Lab of Optical Technology for Microfabrication, Chinese Academy of Science, Chengdu 610029, China

DOI: 10.1109/JPHOT.2012.2216863
1943-0655/$31.00 ©2012 IEEE

Manuscript received August 3, 2012; revised August 24, 2012; accepted August 28, 2012. Date of publication September 7, 2012; date of current version September 13, 2012. This work was supported in part by the National Basic Research Program of China under Grant 2011CB301800, by the Key Grant Project of Chinese Ministry of Education under Grant 313049, by the State Key Lab of Optical Technologies for Micro-Engineering and Nano-Fabrication of China, by the Fundamental Research Funds for the Central Universities under Grant SWJTU11CX136, and by the Funds for the Excellent Ph.D. Dissertation of Southwest Jiaotong University in 2011. Corresponding author: L.-S. Yan (e-mail: lsyan@home.swjtu.edu.cn).

Abstract: *Spectral* characteristics of surface plasmon polaritons (SPPs) in metal–insulator–metal (MIM) waveguides with a rectangular or V-groove are analyzed. Theoretical and simulation results indicate that both schemes can achieve wavelength filtering functionality with the center wavelength possessing a linear relationship with the length of the groove. The plasmonic MIM waveguide with a tilted groove could be regarded as the composition of a hypotenuse, rectangular, and V-shaped structures based on theoretical analyses. Characteristics of such waveguides are further investigated numerically by the finite-different time-domain (FDTD) method. The center wavelength of such structure has a nonlinear relationship with the height of the groove. The unique feature may help researchers design grooves with specified angles in nanophotonic integrated circuits.

Index Terms: Surface plasmon polaritons (SPPs), waveguide, tilted groove, transmission.

1. Introduction

Guiding of light within a subwavelength cross section has recently attracted lots of attentions. The modes guided along the metal/dielectric interface is referred as surface plasmon polaritons (SPPs) [1], which have been considered as one of the most promising solutions to overcome the diffraction limit of optical devices. Different plasmonic structures, such as particles [2], [3], grooves [4]–[6], cavities [7]–[9], and apertures [10], [11], have been designed to cover a variety of applications and enable integration of photonic circuits at the nanoscale. Especially, metal–insulator–metal (MIM) structures based on SPPs have been widely studied due to unique characteristics for controlling wavelengths, including wavelength splitters [12], combiners, or couplers [13]–[15]. For example, a plasmonic gap filter with stub structure or tooth-shaped structure was studied to build SPP mirrors and beam splitters [16]–[20]. In addition, band gaps have also been demonstrated to be available in the MIM plasmonic Bragg reflectors, which consist of periodic insulators or gratings [21], [22].

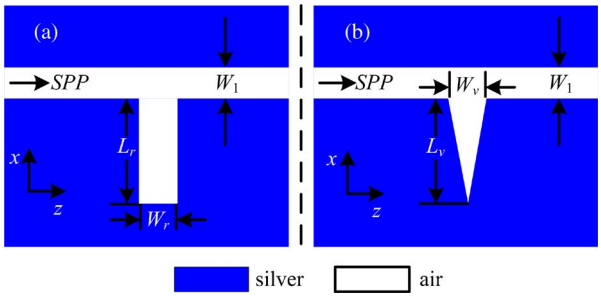

Fig. 1. Scheme of a MIM waveguide with (a) an R-groove and (b) a V-groove.

In [4], a detailed analytic model for a basic MIM waveguide with a single groove is given. The transmission characteristic of such kind of filter has been widely demonstrated to be significantly affected by the heights and the widths of the grooves. The center wavelength (CW) usually exhibits a linear relationship with the height of the groove [4], [17]. It should be pointed out that a tilted groove might arise during the manufacture process, resulting in unknown transmission characteristics. On the other hand, one may benefit from the tilted grooves with specified angles because of potential SPPs manipulation features. Therefore, in this paper, we investigate a generic MIM waveguide with a single groove that has an arbitrary tilted angle. As the length of the groove is fixed, the height of groove is decided by the tilted angle. Subsequently, the height is the only parameter to be varied to study the spectral characteristics in this paper. Theoretical analyses and simulation results based on the finite-different time-domain (FDTD) method demonstrate that this configuration can be performed as a wavelength selection device and the transmission wavelength has a nonlinear relationship with the height of the groove.

2. Theory and Simulation

The scheme of a MIM waveguide with a rectangular groove (R-groove) or a V-groove is shown in Fig. 1. The SPPs propagate along the z-direction inside the MIM plasmonic waveguide. In Fig. 1(a), for a vertical R-groove with a small width W_r, its effective index n can be obtained from the dispersion equation of the TM mode consisting of E_x, E_z, and H_y components in the waveguide given by [23], [24]

$$n = \sqrt{\varepsilon_i - \frac{2\varepsilon_d\sqrt{\varepsilon_d - \varepsilon_m}}{k_0 W_r \varepsilon_m}} \tag{1}$$

where $k_0 = 2\pi/\lambda$ is the propagation constant in the vacuum, W_r is the width of the groove, and ε_i and ε_m are the dielectric constants of air medium and silver, respectively. The transmission wavelength can be expressed as

$$2\pi n_{eff}(2L_r + W_r)/\lambda + \Delta\varphi = 2(m+1)\pi \tag{2}$$

where L_r and W_r are the length and the width of the R-groove, respectively, n_{eff} is the real part of the effective index n, and $\Delta\varphi$ is the phase shift caused by the reflection on the air–silver surface.

However, for the case of V-groove, the transmission wavelength cannot be simply estimated by using (1) and (2). Through integrating the index contrast over the groove depth, we can obtain the phase delay as

$$2\int_0^L \frac{2\pi}{\lambda}\sqrt{\varepsilon_i - \frac{2\varepsilon_d\sqrt{\varepsilon_d - \varepsilon_m}}{k_0 W_v\left(1 - x/\sqrt{L_v^2 + (W_v/2)^2}\right)\varepsilon_m}}\,dx + \sqrt{\varepsilon_i - \frac{2\varepsilon_d\sqrt{\varepsilon_d - \varepsilon_m}}{k_0 W_L \varepsilon_m}}W_L + \Delta\varphi = 2(m+1)\pi \tag{3}$$

where $W_L = W_v(1 - L/\sqrt{L_v^2 + (W_v/2)^2})$, and W_v is the width of the V-groove. It should be noted that L is slightly less than the hypotenuse length to avoid an infinitely sharp bottom tip of the groove.

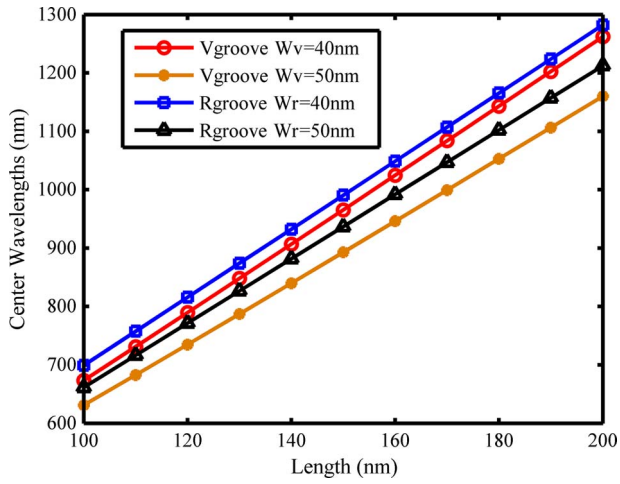

Fig. 2. Theory calculation results: CW versus length of the grooves.

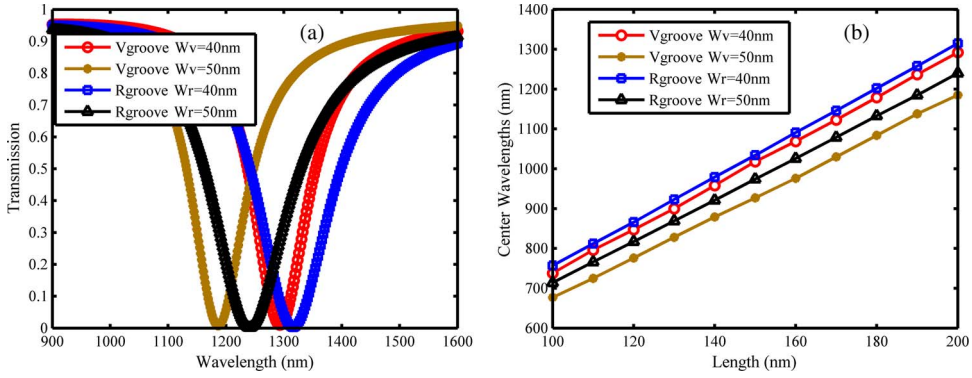

Fig. 3. (a) Transmission spectra of the R-groove and V-groove waveguides (b) Center wavelength versus length of the groove.

In the following calculation, the frequency-dependent complex relative permittivity of silver is characterized by the Drude model

$$\varepsilon_m(\omega) = \varepsilon_\infty - \omega_p^2/\omega(\omega + i\gamma) \tag{4}$$

where $\omega_p = 1.38 \times 10^{16}$ Hz stands for the bulk plasma frequency, $\gamma = 2.73 \times 10^{13}$ Hz is the electron collision frequency, ω is the angular frequency of the incident electromagnetic radiation, and ε_∞ is the dielectric constant at infinite angular frequency with the value of 3.7 [21].

According to (2) and (3), we can estimate the transmission wavelength. By fixing the widths of the R- and V-grooves, i.e., 40 nm or 50 nm, we can see that the CWs have a linear relationship with the groove lengths, as shown in Fig. 2. Moreover, the CWs of the V-groove MIM waveguide are always less than those of the R-groove MIM waveguide when their widths and lengths are identical, respectively.

To further study the transmission spectra, we use FDTD simulation tools (Lumerical FDTD Solutions 7.5.7) to characterize the SPPs propagation under perfect-matching-layer (PML) absorbing boundary conditions. The mesh accuracy is set to be 1 nm, and the incident light is defined as a plane wave. Moreover, the tabulation of the optical constants of silver [25] is used. From Fig. 3(a), it can be seen that band gaps are available in both cases of the MIM waveguides composing of an R- or a V-groove, whose lengths are identical, i.e., $L_r = L_v = 200$ nm. The troughs with the transmittance $\sim$0 occur at the free-space wavelength of about 1315 nm or 1240 nm, and 1293 nm or 1186 nm for the R-groove and the V-groove when width is 40 nm or 50 nm, respectively.

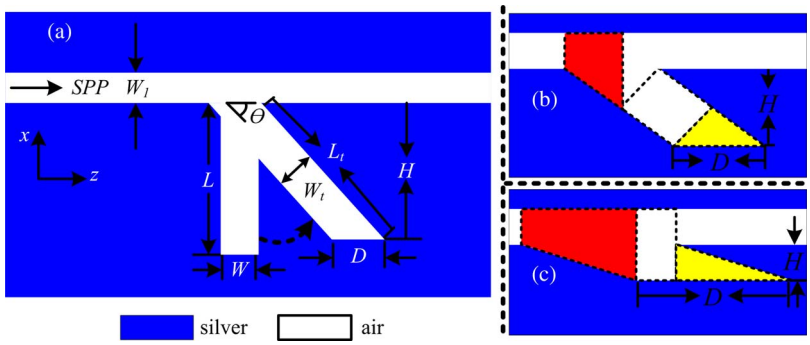

Fig. 4. (a) Schematic diagram of the MIM waveguide with a tilted groove, (b) and (c) are the equivalent models of the tilted groove.

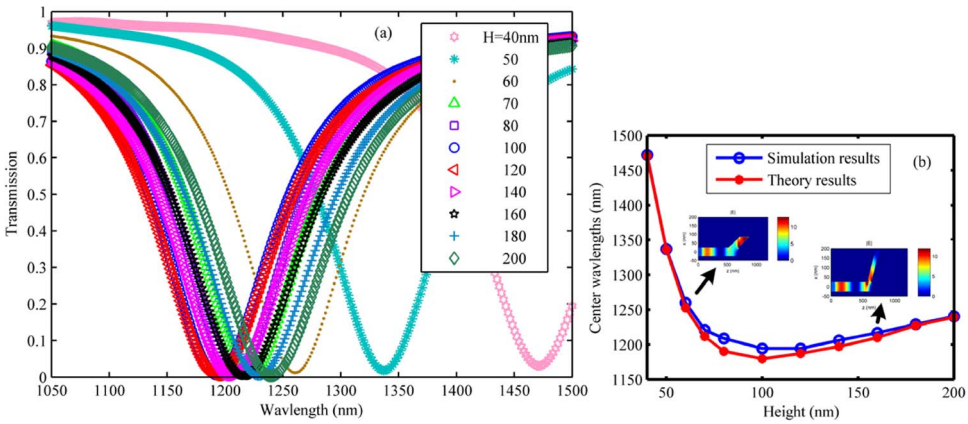

Fig. 5. (a) Simulation results of transmission spectra (b) Calculated and simulated CWs as a function of the height of the groove.

TABLE 1

Center wavelengths of simulation and theoretical results

H (nm)	θ (^{0})	CWs (nm)		H (nm)	θ (^{0})	CWs (nm)	
		Simulation	Theory			Simulation	Theory
200	90.0	1240.1	1239.1	80	23.6	1208.7	1190.1
180	64.2	1229.0	1227.2	70	20.5	1220.8	1211.8
160	53.1	1216.7	1210.0	60	17.5	1260.1	1252.6
140	44.4	1206.0	1197.1	50	14.5	1337.0	1336.3
120	36.9	1194.2	1187.1	40	11.5	1171.7	1170.4
100	30.0	1194.1	1179.5				

Fig. 3(b) further demonstrates that the transmission CWs increase linearly with the groove lengths. Comparing to Fig. 2, simulated results in Fig. 3(b) are slightly larger than theoretical ones for the reason that the phase shift $\Delta\varphi$ is ignored during analyses.

Based on the above analyses, we further study the MIM waveguide with a tilted groove, as shown in Fig. 4(a). Such tilted groove might be raised during the manufacture process, resulting in

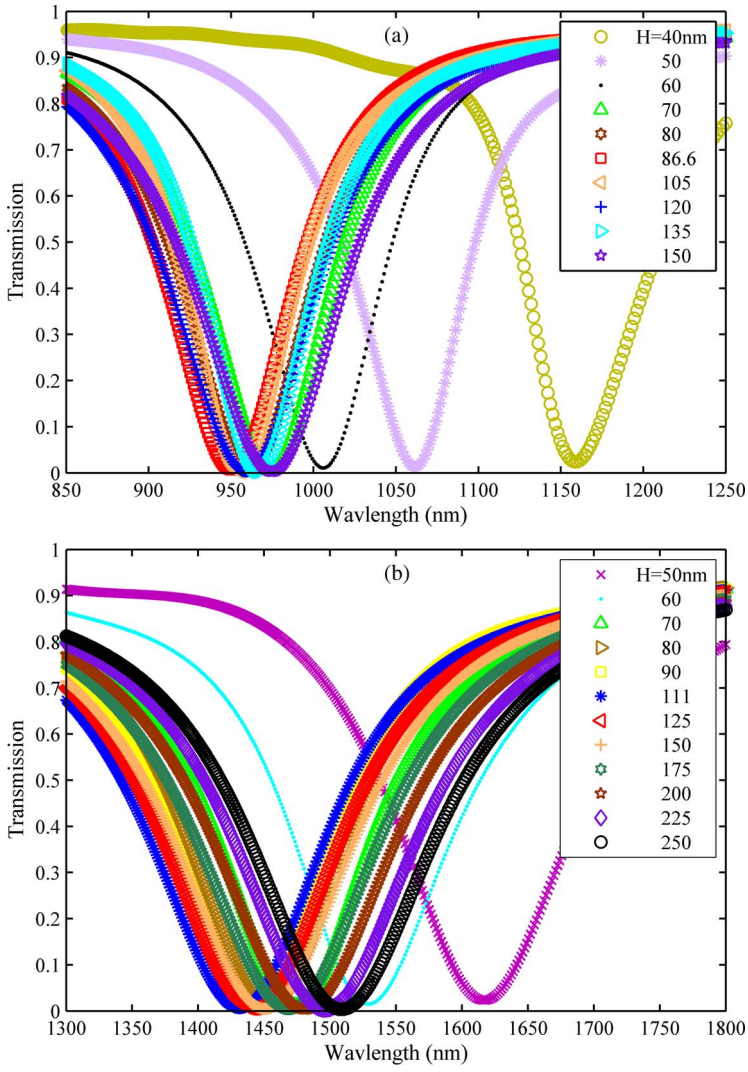

Fig. 6. Transmission spectra of the tilted groove with different heights and (a) $L_t = 150$ nm, and (b) $L_t = 250$ nm.

unknown transmission characteristics. Therefore, it is necessary to study the SPP transmission characteristic for such kind of structures. In the following analyses and simulations, the width and the length of the groove are fixed, i.e., $W = W_t$ and $L = L_t$.

In terms of the tilted angle, two equivalent models are proposed to study the SPP propagation phase delay, as shown in Fig. 4(b) and (c), both of which can be modeled as a composition of hypotenuse-shaped (red), rectangular-shaped (white) and V-shaped (yellow) structures. Specifically, the tilted groove can be separated into three parts, and the phase delay in the rectangular part can be calculated by using (2), while for the hypotenuse-shaped part and V-shaped part, it is calculated by using the method of (3). The total phase delay satisfies

$$\phi = \int_{W_1}^{L_1} k_0 n_{eff1}(x)dx + 2n_{eff2}L_2 + 2\int_0^{L_3} k_0 n_{eff3}(x)dx + \Delta\varphi = 2(m+1)\pi. \quad (5)$$

In Fig. 4(b), $L_1 = W_1 + W_t\cos\theta$, $L_2/\sin(\theta) = H - (L_1 - W_1)$, and $L_3 < D$, and in Fig. 4(c), $L_1 = W_1 + H$, and $L_2 + L_3 < D$, where $D = W_t/\sin(\theta)$ is the side length of the groove, and $H = L_t\sin(\theta)$ is

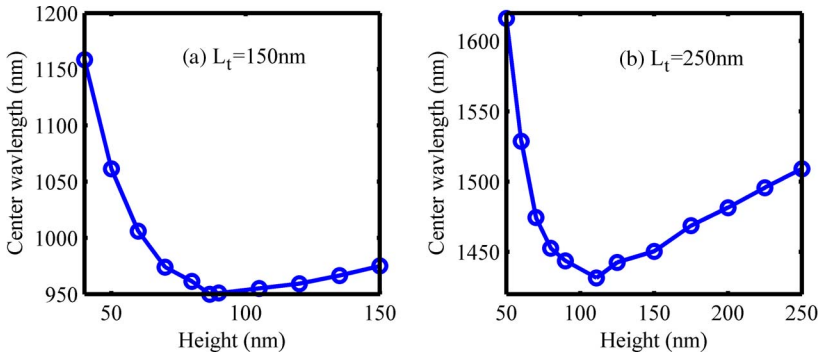

Fig. 7. Center wavelength versus height of the tilted groove waveguide with (a) $L_t = 150$ nm, and (b) $L_t = 250$ nm.

the height of the groove. The simulation parameters are defined as $W = W_t = 50$ nm and $L = L_t = 200$ nm. When the height of the groove H is larger than its side length D, Fig. 4(b) is the appropriate model. Otherwise, Fig. 4(c) is used to analyze the structure. Obviously, the height of the groove H is decided by the tilting angle as the length of the groove is fixed. Thus, in the following simulation and analyses, the height is the only parameter to be varied.

Fig. 5(a) indicates that the MIM waveguide with a tilted groove also has the filtering characteristics with the CWs significantly affected by the height (i.e., tilted angle). The transmittances for all the troughs are about 0, which can be investigated by the electric-field intensity |E| in Fig. 5(b). In addition, the simulated and analytical results in Fig. 5(b) also reveal the variations of the CWs. As the height decreases, the CWs first decrease linearly for the reason that the groove contains a small V-shaped structure (see Fig. 2) and then increase nonlinearly because of the nonlinearly increase of the side length D. The inflection point of the CWs variation curve arises when the side length D is equal to the height H, i.e., the minimum wavelength is available when $D = H$. In this case, as $H = L_t \sin(\theta)$ and $D = W_t/\sin(\theta)$, thus, we can obtain $D = H = 100$ nm and $\theta = 30^\circ$. The results are shown in Table 1 in details.

To further investigate the spectral characteristics, we set the length of the tilted groove L_t to be 150 nm or 250 nm. The heights of the groove H are in the ranges of 40 nm to L_t. The simulation results based on FDTD method in Fig. 6(a) and (b) show that the band gaps are always available at different CWs that have similar performance to that of the groove with $L_t = 200$ nm, i.e., decrease linearly firstly and then increase nonlinearly as the height decreases. The minimum wavelength 950 nm arises when $D = H = 86.6$ nm and $\theta = 35.3^\circ$, as shown in Fig. 7(a), or the minimum wavelength 1431.6 nm arises when $D = H = 111.8$ nm and $\theta = 26.6^\circ$ as shown in Fig. 7(b).

3. Conclusion

In this paper, we have investigated a MIM waveguide with a tilted groove as a wavelength filter. Under fixed width and length of the groove, the CW of the band gap has a nonlinear relationship with the height H of the groove. Such configuration may provide an alternate approach for designing wavelength selection devices in nanophotonic integration.

References

[1] W. L. Barnes, A. Dereux, and T. W. Ebbesen, "Surface plasmon subwavelength optics," *Nature*, vol. 424, no. 6950, pp. 824–830, Aug. 2003.
[2] S. A. Maier, P. G. Kik, H. A. Atwater, S. Meltzer, E. Harel, B. E. Koel, and A. G. Requicha, "Local detection of electromagnetic energy transport below the diffraction limit in metal nanoparticle plasmon waveguides," *Nat. Mater.*, vol. 2, no. 4, pp. 229–232, Mar. 2003.
[3] W. H. Weber and G. W. Ford, "Propagation of optical excitations by dipolar interactions in metal nanoparticle chains," *Phys. Rev. B*, vol. 70, no. 12, pp. 125 429-1–125 429-8, Sep. 2004.

[4] X.-S. Lin and X.-G. Huang, "Tooth-shaped plasmonic waveguide filters with nanometeric sizes," *Opt. Lett.*, vol. 33, no. 23, pp. 2874–2976, Dec. 2008.
[5] S. I. Bozhevolnyi, V. S. Volkov, E. Devaux, and T. W. Ebbesen, "Channel plasmon-polariton guiding by subwavelength metal grooves," *Phys. Rev. Lett.*, vol. 95, no. 4, pp. 046802-1–046802-4, Jul. 2005.
[6] A. Krishnan, L. Grave de Peralta, M. Holtz, and A. A. Bernussi, "Finite element analysis of lossless propagation in surface plasmon polariton waveguides with nanoscale spot-sizes," *J. Lightw. Technol.*, vol. 27, no. 9, pp. 1114–1121, May 2009.
[7] Q. Zhang, X.-G. Huang, X.-S. Lin, J. Tao, and X.-P. Jin, "A subwavelength coupler-type MIM optical filter," *Opt. Exp.*, vol. 17, no. 9, pp. 7549–7555, Apr. 2009.
[8] J. C. Weeber, A. Bouhelier, F. G. Des, L. Markey, and A. Dereux, "Submicrometer in-plane integrated surface plasmon cavities," *Nano Lett.*, vol. 7, no. 5, pp. 1352–1359, May 2007.
[9] F. F. Hu, H. X. Yi, and Z. P. Zhou, "Wavelength demultiplexing structure based on arrayed plasmonic slot cavities," *Opt. Lett.*, vol. 36, no. 8, pp. 1500–1502, Apr. 2011.
[10] C. Janke, J. Gómez Rivas, P. Haring Bolivar, and H. Kurz, "All-optical switching of the transmission of electromagnetic radiation through subwavelength apertures," *Opt. Lett.*, vol. 30, no. 18, pp. 2357–2359, Sep. 2005.
[11] M. J. Kofke and D. H. Waldeck, "The effect of periodicity on the extraordinary optical transmission of annular aperture arrays," *Appl. Phys. Lett.*, vol. 94, no. 2, pp. 023104-1–023104-3, Jan. 2009.
[12] G. Veronis and S. Fan, "Bends and splitters in metal–dielectric–metal subwavelength plasmonic waveguides," *Appl. Phys. Lett.*, vol. 87, no. 13, pp. 131102-1–131102-3, Sep. 2005.
[13] H. Gao, H. Shi, C. Wang, C. Du, X. Luo, Q. Deng, Y. Lv, X. Lin, and H. Yao, "Surface plasmon polaritons propagation and combination in Y-shaped metallic channels," *Opt. Exp.*, vol. 13, no. 26, pp. 10795–10800, Dec. 2005.
[14] H. Y. Li, X. G. Luo, L. S. Yan, K. H. Wen, Z. Guo, and J. Chen, "Polarization and transmission properties of metamaterial-based three-dimensional plasmonic structure," *IEEE Photon. J.*, vol. 3, no. 3, pp. 400–406, Jun. 2011.
[15] R. A. Wahsheh, Z. Lu, and M. A. G. Abushagur, "Nanoplasmonic couplers and splitters," *Opt. Exp.*, vol. 17, no. 21, pp. 19033–19040, Oct. 2009.
[16] A. Pannipitiya, I. D. Rukhlenko, M. Premaratne, H. T. Hattori, and G. P. Agrawal, "Improved transmission model for metal–dielectric–metal plasmonic waveguides with stub structure," *Opt. Exp.*, vol. 18, no. 6, pp. 6191–6204, Mar. 2010.
[17] J. Tao, X. G. Huang, X. S. Lin, J. H. Chen, Q. Zhang, and X. P. Jin, "Systematical research on characteristics of double-sided teeth-shaped nanoplasmonic waveguide filters," *J. Opt. Soc. Amer. B*, vol. 27, no. 2, pp. 323–327, Feb. 2010.
[18] Y. H. Guo, L. S. Yan, W. Pan, B. Luo, K. H. Wen, Z. Guo, H. Y. Li, and X. G. Luo, "A plasmonic splitter based on slot cavity," *Opt. Exp.*, vol. 19, no. 15, pp. 13 831–13 838, Jul. 2011.
[19] I. Chremmos, "Magnetic field integral equation analysis of surface plasmon scattering by rectangular dielectric channel discontinuities," *J. Opt. Soc. Amer. A, Opt. Image Sci. Vis.*, vol. 27, no. 1, pp. 85–94, Jan. 2010.
[20] K. H. Wen, L. S. Yan, W. Pan, B. Luo, Z. Guo, and Y. H. Guo, "Wavelength demultiplexing structure based on a plasmonic metal–insulator–metal waveguide," *J. Opt.*, vol. 14, no. 7, p. 075001, Jul. 2012.
[21] Z. H. Han, E. Forsberg, and S. L. He, "Surface plasmon Bragg gratings formed in metal–insulator–metal waveguides," *IEEE Photon. Lett.*, vol. 19, no. 2, pp. 91–93, Jan. 2007.
[22] B. Wang and G. P. Wang, "Plasmon Bragg reflectors and nanocavities on flat metallic surfaces," *Appl. Phys. Lett.*, vol. 87, no. 1, pp. 013107-1–013107-3, Jul. 2005.
[23] J. A. Dionne, L. A. Sweatlock, and H. A. Atwater, "Plasmon slot waveguides: Towards chip-scale propagation with subwavelength-scale localization," *Phys. Rev. B*, vol. 73, no. 3, pp. 035407-1–035407-9, Jan. 2006.
[24] S. I. Bozhevolnyi and J. Jung, "Scaling for gap plasmon based waveguides," *Opt. Exp.*, vol. 16, no. 4, pp. 2676–2684, Feb. 2008.
[25] P. B. Johnson and R. W. Christy, "Optical constants of the noble metals," *Phys. Rev. B*, vol. 6, no. 12, pp. 4370–4379, Dec. 1972.